

Identification of Luminal and Medial Adventitial Borders in Intravascular Ultrasound Images Using Level Sets

Ali Iskurt, Sema Candemir, and Yusuf Sinan Akgul

GIT Vision Lab
Gebze Institute of Technology
Department of Computer Engineering,
Gebze, Kocaeli, Turkey
{iskurtali, scandemir, akgul}@bilmuh.gyte.edu.tr
<http://www.bilmuh.gyte.edu.tr>

Abstract. Extraction of the media and plaque boundaries from the intravascular Ultrasound (IVUS) images is gaining popularity as a biomedical application. This paper presents a novel system for the fully automatic extraction of the boundaries of the media and the plaque visible in the IVUS images. The system utilizes an enhanced level set technique to derive the evolution of two coupled contours as the zero level sets of a single higher dimensional surface. Moreover, the system utilizes the surface features to impose the expected media thickness. By using the single surface as a communication path between the contours, the system carries all the advantages of using two evolving surfaces and it becomes more efficient, less complex, easily extensible, and faster. Additionally, the capability of using different dynamic behaviors for the segmentation of the inner and outer walls makes our system even more flexible. The derived surface evolution equations capture the domain dependent information in an elegant and effective manner and address many practical issues, such as the missing wall sections or very weak boundary contrast. We have verified the accuracy and effectiveness of our system on synthetic and real data.

1 Introduction

Intravascular ultrasound (IVUS) is a relatively new medical imaging technique which can provide information complementary to angiography. An ultrasound transducer on the tip of a catheter provides cross-sectional images of the coronary arteries, which produces the morphological views of both the plaque and the arterial wall as shown in Fig.1. It has been shown that IVUS can demonstrate[10] diseases in cases where angiography is misleading proper coronary therapy[9]. Geometric information about the lumen, plaque, and vessel wall can be easily obtained by IVUS. In addition, IVUS can supply crucial data about the plaque type which is really important for the identification of sections of vessels likely to rupture. As a result, IVUS is becoming a popular technique for direct visualization of the coronary arteries.

Traditionally, the manual analysis of IVUS images is laborious, time consuming, and subject to large interobserver and intraobserver variability which prevents us from taking the full advantages of IVUS technology. Computerized segmentation of IVUS images will address these problems since the results will be objective. It will not require intense manual intervention and the overall cost will be less.

There are a number of techniques for the semi-automatic segmentation of IVUS images. An overview of the common 2-D and 3-D segmentation and reconstruction systems was presented in [4]. One classical approach is the 3D segmentation of Li *et al.*[11], which performs both longitudinal and cross-sectional semiautomatic contour detection based on a minimum cost algorithm. This algorithm was performed in clinical applications by von Birgelen *et al.*[2]. Knowledge-based solutions was proposed by Sonka *et al.*[6] and this research soon led to 3D modeling using this [1]. This segmentation is based on a graph-search approach within a manually determined elliptical region of interest(ROI). Despite the popularity of IVUS, there are no fully automatic systems available.

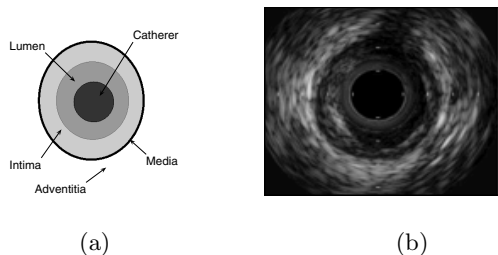


Fig. 1. (a) The layers of a coronary artery wall. (b) An intravascular ultrasound image.

This paper presents a novel technique for the segmentation of the IVUS images. The technique is based on evolving two contours with different dynamics and stopping them with the constraint of media thickness and uniquely address many IVUS specific problems. If one of the image boundaries is missing or has weak image contrast, the information obtained from other contour can be employed to find the expected position. Similarly, if both contours have missing image data, the system can impose a media thickness constraint on the boundary position to come up with an estimate. This property is especially useful for obtaining media segment in IVUS images.

Among all other techniques for the segmentation of images in Computer Vision, level sets method is utilized in our research because of the advantages they offer. First, it is very easy in the level set theory to go to an upper dimension. Thus, once the 2D image segmentation is formulated, it will be straightforward to use it in the 3D reconstruction of a vessel. Second, it is possible to impose constraints in level sets for special case studies like IVUS. For instance, one constraint will be the media thickness. Levels set methods have already been applied

to 3D medical image segmentation[3], detection of vessel borders in magnetic resonance angiography (MRA) images[5], segmentation of white and gray matters in MRI images[13] and many other areas.

The straightforward usage of level sets was not applicable for IVUS image segmentation. Therefore, level set theory had to be refined to capture the IVUS related constraints and to address the emerging problems. Thus, we extend the classical level set framework in several novel ways. The zero set contours of a single three dimensional surface would correspond to the inner and outer wall boundaries. The surface movement along the normal direction moves the boundaries towards each other and the inherent geometric constraints on the surface makes the contours keep a distance that enforces a thickness constraint of the media. The local surface properties, such as the directional surface derivatives, make it possible to elegantly define different evolution behaviors for the two contours.

Rest of this paper is organized as follows. Section 2 provides information about how we refine classical level set methods and the novel extensions that we introduce with this paper. The experiments on system validation on synthetic images under varying controlled noise and anomalies are explained in Section 3. Section 3 also includes the experiments performed on real IVUS data. Finally, we provide concluding remarks in Section 4.

2 Segmentation

Our system is based on two deformable contours evolving on the IVUS images. To drive the contour evolutions, we make use of the level set methods which were introduced[7] to Computer Vision for recovering shapes of objects in two or three dimensions. The basic idea of level set methods is to embed the shape of the objects as the zero level set of a higher dimensional surface. While the surface evolves, the zero level set contours might develop singularities and sharp corners or they might change topology. Finally, contour evolution stops at desired boundaries.

The contours are evolved in a way that they try to move smoothly towards each other while seeing some resistance from the image features at likely boundary positions. The two contours are not allowed to come too close or stay too far from each other. At the end of the deformations, the inner and outer media boundaries are localized.

Consider two time-dependent, i.e. moving, closed contours $c_1(t)$ and $c_2(t)$ on R^2 . The contours c_1 and c_2 never intersect and c_1 is always inside c_2 for $t \geq 0$. Our motivation is to use the contours c_1 and c_2 to extract the inner and outer walls of media. We will write the motion equations for these contours that will move them towards the wall boundaries and stop them when the destination is reached.

Let C be the set of points on $c_1(0)$ and $c_2(0)$. Consider a function s ,

$$s(\mathbf{x}) = \begin{cases} 0, & \text{if } \mathbf{x} \in C; \\ -d(x), & \text{if } \mathbf{x} \text{ is outside } c_1(0) \text{ but inside } c_2(0); \\ d(x), & \text{otherwise,} \end{cases} \quad (1)$$

where d is the shortest distance to C from point $\mathbf{x} \in R^2$. We define the time dependent surface $\varphi(\mathbf{x}, t = 0)$ by

$$\varphi(\mathbf{x}, t = 0) = G(\alpha|s(\mathbf{x})|) * s(\mathbf{x}), \quad (2)$$

where $G(\sigma)$ is the two dimensional Gaussian with variance σ^2 , $\alpha > 0$ is a weighting constant, and $*$ is the standard convolution operation. Note that when $\mathbf{x} \in C$, the surface φ is the same as the function s because the σ of the Gaussian function becomes zero at those points. Note also that Equation (2) implies that

$$C = \{\mathbf{x} | \varphi(\mathbf{x}, t = 0) = 0\}. \quad (3)$$

The original idea of level sets is to define a smooth higher dimensional function that represents the lower dimensional contours (the interface or the front) to be extracted/tracked as the zero level set of the higher dimensional function. If we take the intersection of the X-Y plane with the function $\varphi(\mathbf{x}, t = 0)$, the two closed contours $c_1(0)$ and $c_2(0)$ are obtained (See Fig. 2). We would like to expose the surface φ to a velocity field that depends on geometry, position, and image data. While φ moves under the influence of the velocity field, the contours c_1 and c_2 also move to find the desired wall boundaries.

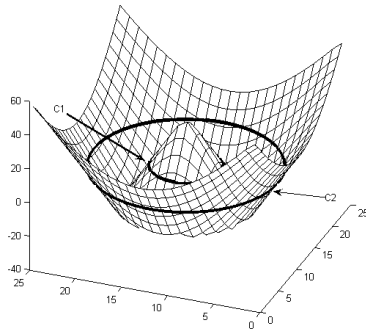


Fig. 2. The surface φ at $t = 0$. The zero level set of φ produces the contours c_1 and c_2 .

The elementary equation of motion under the velocity field can be written[8] as

$$\frac{\partial \varphi}{\partial t} + V|\nabla \varphi| = 0, \quad (4)$$

where V is the normal component of the desired velocity of the front and $|\nabla \varphi| = \sqrt{\frac{\partial \varphi^2}{\partial x} + \frac{\partial \varphi^2}{\partial y}}$.

Furthermore, the geometric properties of the contours c_1 and c_2 (the front), such as the normal or the mean curvature, can easily be calculated from the surface. The normal to the front is simply the gradient of the surface, $\nabla\varphi$. The mean curvature of the front can be conveniently obtained by

$$\kappa = -\nabla \frac{\nabla\varphi}{|\nabla\varphi|}. \quad (5)$$

We recognize that the normal vectors of the points on $c_1(t)$ and $c_2(t)$ have opposite directions. If the velocity field contains constant velocity values for all points, then we expect the contour c_1 to expand and c_2 to shrink according to the Equation 4. This is a desirable feature of our design of the level set function because our motivation of using coupled dual contours is to obtain a contour movement that pushes the contours together until they find the correct boundaries. This natural movement of the surface φ governed by the Equation 4 greatly simplifies our system both in terms of mathematical complexity and computational efficiency. Other systems that use levels sets to perform multiple contour extraction, such as Yezzi *et al.*[12], use more than one evolving surface.

We need a mechanism for stopping the contours when they are close to the desired borders. We also need to establish a communication path between these contours so that they would stop moving if they come too close when there is no image feature to stop them. The next section describes how we use the image data and surface geometry information to achieve this goal.

2.1 Recovering the Boundaries

We would like to define a velocity function that takes the image data into account so that the moving contours c_1 and c_2 would stop at the boundaries. We follow the notation of Malladi *et al.*[7] and separate the velocity function into two additive components. We will keep the advection term component, V_A , so that the two contours are pushed towards each other. The other component, V_G depends on the geometry of the front. It smoothes out the high curvature sections of the front and is defined by Equation 5. The velocity function we have is

$$V = k_I k_G (V_A + V_G), \quad (6)$$

where k_I and k_G are multiplicative terms each of which can stop the surface evolution if they become zero. In our implementation, each of the four terms have weighting constants to adjust the influence of the term on the overall velocity. The weighting constants were removed from the formula for the presentation clarity.

If portions of the image data is missing or very weak as in IVUS, boundaries will be localized incorrectly. For correct localization the thickness constraint is utilized by looking at the ridges between the contours in spatial gradient. For obtaining spatial gradient, we look at φ which is differentiable even around the minima points between the contours c_1 and c_2 , so the partial derivatives of φ with respect to x and y should vanish around the minima points, which should

make the spatial gradient $|\nabla\varphi|$ values close to zero around the vicinity of the extrema region. This idea is incorporated into the multiplicative velocity term k_G at \mathbf{x} as

$$k_G(\mathbf{x}) = \begin{cases} 0, & \text{if } |\nabla\varphi(\mathbf{x})| < \gamma \text{ and } \varphi(\mathbf{x}) < 0; \\ |\nabla\varphi(\mathbf{x})| - \gamma, & \text{otherwise,} \end{cases} \quad (7)$$

where $\gamma > 0$ is a constant. k_G will slow down the contour movement when the contours get close and depending on the γ value, it will stop the contour evolution completely. Note that $|\nabla\varphi|$ also vanishes for the center region of the inner contour, which can be dealt with by checking the sign of the surface height.

Note that if we let the surface φ evolve on a flat image with no features, the contours c_1 and c_2 will be attracted towards each other but they will never collide due to the multiplicative velocity term k_G . There will be a distance between the contours at the end of the evolution process and this distance depends on the α value of Equation 2 and γ value of Equation 7. In other words, the α and γ values are parameters that directly affect the extracted media thickness. The ability of accepting expected media thickness is a flexible feature for a practical system because it allows one to input beneficial data to the system for extra robustness.

Even though the evolutions of both media contours are strongly tied to the same 3D surface evolution, our formulations allow different evolution characteristics for each contour in an elegant way. Formally, checking the signs of the directional derivatives of the surface towards the highest surface position inside the inner contour will give us the information about which boundary that point belongs. The sign to check for this information can be calculated using

$$\text{sign}(\nabla\varphi(\mathbf{x}) \cdot \mathbf{x}). \quad (8)$$

The information produced by equation 8 is valuable for a number of applications that can define different properties for the inner and outer boundaries. In IVUS data, inner walls has better contrast and can easily be identified. It is preferable to give more weight to easily identified sections and let this information affect the other boundary extraction, which can be achieved in our system by simply choosing different weights for the inner and outer contours image velocity components.

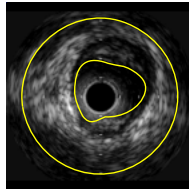


Fig. 3. Lumen-intima interface captured

Using the above mechanism, we first evolve the inner contour and capture the lumen-intima interface as shown in Fig.3. During this evolution, outer contour stands still which is seen as the blue contour. Then, we evolve the inner contour to outer side for a few pixels with normal velocity without the influence of the image. The inner contour now left the lumen-intima wall behind and can go on evolving for finding the media segment together with outer contour. At this time, image gradient features are not permitted to be dominant over the geometry term that imposes thickness constraints. We also increase the influence of the curvature term. This is because we expect a ring-like structure in the end and do not want the contours to be influenced by non-circular gradients. At the end of the surface evolutions, the two level set contours will find the high gradient contour regions that are separated by a distance of certain thickness.

3 Experiments and Validation

We validated the system using both synthetic data and real IVUS images. Synthetic images are used for the quantitative evaluation of the system. The real IVUS images validated the system in the real world.

3.1 Localization of Circular Structure

In order to test the ability for correctly extracting a ring structure with a certain width in a noisy environment, synthetic test images are used. Like the IVUS images, test images are not of very high quality and they contain artifacts. Moreover, the images have missing ring sections. The types of noise added were chosen to reflect the problems seen in IVUS images. Zero mean Gaussian, speckle, and salt & pepper noise types are added to the images with varying amounts.

Fig. 4 shows a few examples of the images used in the experiments. The images are about 100 by 100 pixels in size and the object has a contrasts of

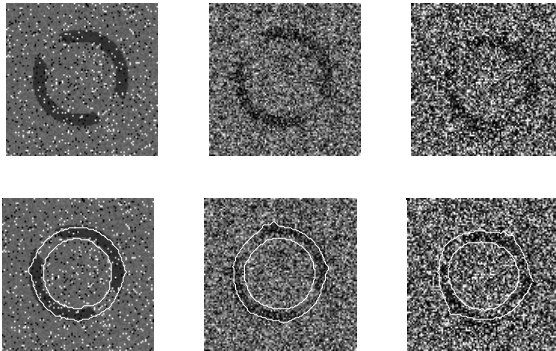


Fig. 4. Example synthetic images used for testing are shown at the top row. The bottom row shows the automatically extracted contours by our system for the same images.

50 gray levels. The wall extraction system produced two ring boundaries, which were compared to the ground truth contours that were used to produce the synthetic images. Table. 1 and Fig. 5 show the error values measured under changing noise and artifact conditions. We observe from the error data that our system performs very well even under high amounts of noise and artifacts. We are especially encouraged by the handling of missing wall sections.

Table 1. Noise Levels and Average Pixel Errors

	1	2	3	4	5	6	7	8	9	10	11	12
Gaussian (σ^2)	0	0	0.01	0	0.02	0.02	0.05	0.08	0.15	0.2	0.3	0.3
Salt and Pepper (%)	0	0	0	0	2	2	5	5	8	10	10	20
Speckle (σ_λ^2)	0	0	0	0	0	0	0.05	0.1	0.1	0.1	0.1	0.2
Missing Walls (%)	0	5	0	15	0	5	15	15	15	20	20	20
Average Pixel Error	0.95	1.03	1.37	1.42	1.82	2.15	2.22	2.58	3.00	3.16	3.67	4.09

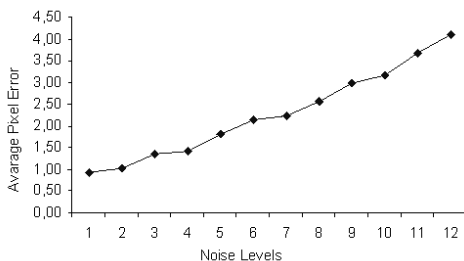


Fig. 5. The graph of the error values for Fig. 1

3.2 Application to Intravascular Coronary Ultrasound

The boundaries of the artery walls, which yields crucial information about the artery blockages, are obtained from the fully automatic segmentation of the IVUS images. The artery wall consists of three layers: intima, media, and adventitia (see Fig. 1-a). The interface between lumen and intima is referred as inner wall and the interface between media and adventitia is defined as the outer vessel wall. IVUS images are ring-shaped, not very contrasty and not clean around the artery wall sections(see Fig. 1-b).

We have applied our segmentation mechanism on various IVUS images of different patients and obtained very satisfying results. Since it is not possible to produce ground truth for the real IVUS images, we validated our results visually. Figure 6 shows only the results for two of them. We automatically removed the catheter boundaries from the image during the experiments. As can be seen in the IVUS images, the inner vessel wall has a better contrast and it should lead the extraction of the outer boundary.

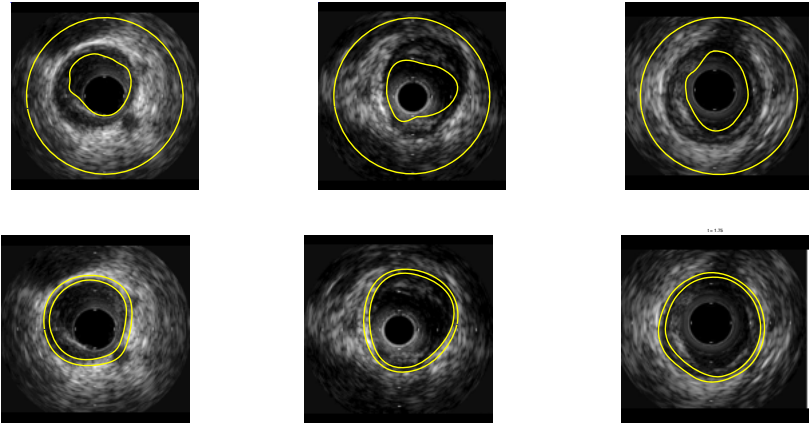


Fig. 6. Lumen-intima interfaces at images on top . Media segments of the same images at bottom.

The top three images in Fig.6 show the extracted lumen-intima interfaces. Both images have wide intima regions and narrower lumen regions. On the left-most image, plaque formation is obviously visible at 6 to 12 o'clock position and on the middle image it is visible at 12 to 3 o'clock position. Intima is thin only at 12 to 2 o'clock position in the leftmost image. At the bottom images in Fig.6, it can be observed that media segments are truly captured by double contours. As the visual results show, our system performs as expected and correctly finds the vessel walls and the plaque regions. We are working on obtaining several contours produced manually by experts to compare our results numerically.

4 Conclusions

We presented a Computer Vision system that extracts the inner and outer boundaries of vessels simultaneously in IVUS images. The system captures many domain dependent constraints without using any complicated rule sets or hard constraints. We introduced several novel ideas that make our system computationally efficient, robust against the imaging problems, and flexible to use in practice. At the center of our system, there is a single evolving surface whose zero level set contours represent the wall boundaries. The natural dynamics of our system push the contours together until they find the destination, which makes our system simple but powerful. The contours can evolve under different criteria without complicating the surface evolution mechanism. Another novel feature of our system models the expected thickness of the media by using the evolving surface geometry to decide if the approximate media thickness is reached. This feature is very effective for the missing sections of the media.

We have validated our system by applying it to synthetic and real images. Synthetic localization experiments showed our system's accuracy under controlled

varying conditions with the thickness constraint. Application to IVUS images proved that our method can be used in segmenting images of vessels with a considerable success.

As for the future research, we are actively working on the extensions of this work towards 3D boundary recovery and 2D + time analysis of video sequences. Specifically, we employ IVUS image sequences while the catheter is being pulled inside the vessel. This 3D analysis of IVUS images produce a better and more reliable information about the possible plaque.

Acknowledgements

The authors thank Dr.Bekir Sitki Cebeci and Dr.Lutfi Hocaoglu for providing the IVUS images.

References

1. S. A.Wahle, G.P.M.Prause and M.Sonka. Geometrically correct 3-d reconstruction of intravascular ultrasound images by fusion with biplane angiographymethods and validation. *IEEE Transactions on Medical Imaging*, 18(8), 1999.
2. W. L. J. C. H. S. C. J. S. P. J. d. F. J. R. T. C. R. C. von Birgelen, C. Di Mario and P. W. Serruys. Morphometric analysis in three-dimensional intracoronary ultrasound: An in-vitro and in-vivo study performed with a novel system for the contour detection of lumen and plaque. *American Heart Journal*, 132:516–527.
3. T. Deschamps, R. Malladi, and I. Ravve. Fast evolution of image manifolds and application to filtering and segmentation in 3d medical images. *IEEE Transactions on Visualization and Computer Graphics*, 10(5):525–535, 2004.
4. G. K. J. H. C. R. J. Dijkstra, A. Wahle and M. Sonka. Quantitative coronary ultrasound: State of the art. *Whats New in Cardiovascular Imaging? (Developments in Cardiovascular Medicine) J. H. C. Reiber and E. E. van der Wall Eds. Dordrecht, The Netherlands: Kluwer*, 204:79, 1998.
5. C. Jian and A. Amini. Quantifying 3-d vascular structures in mra images using hybrid pde and geometric deformable models. *IEEE Transactions of Medical Imaging*, 23(10):1251–1262, 2004.
6. M. S. M. S. B. S. C. D. S. M. M. Sonka, X. Zhang and C. R. McKay. Segmentation of intravascular ultrasound images: A knowledge-based approach. *IEEE Transactions on Medical Imaging*, 14:719–732.
7. R. Malladi, J. Sethian, and B. Vemuri. Shape modeling with front propagation: A level set approach. *IEEE Transactions on Pattern Analysis and Machine Intelligence*, 17(2), February 1995.
8. S. Osher and N. Paragios. *Geometric Level Set Methods in Imaging, Vision, and Graphics*. Springer, 2003.
9. C. S. J. B. R. Blasini, F. J. Neumann and A. Schomig. Comparison of angiography and intravascular ultrasound for the assessment of lumen size after coronary stent placement: Impact of dilation pressures. *Cathet. Cardiovasc. Diagn.*, 42:113, 1997.
10. E. J. Topol and S. E. Nissen. Our preoccupation with coronary luminology. the dissociation between clinical and angiographic findings in ischemic heart disease. *Circulation*, 92:2333, 1995.

11. C. D. M. E. E. N. d. P. W. Li, C.vonBirkelen and N.Bom. Semi-automatic contour detection for volumetric quantification of intravascular ultrasound. In *Proc. Computers in Cardiology 1994: IEEE-CS Press*, pages 277–280, Los Alamitos, CA, 1994/95.
12. A. Yezzi, Jr., A. Tsai, and A. Willsky. A fully global approach to image segmentation via coupled curve evolution equations. *Journal of Visual Communication and Image Representation*, 13(1/2):195–216, March 2002.
13. X. S. Zhou, A. Gupta, and D. Comaniciu. An information fusion framework for robust shape tracking. *IEEE Transactions on Pattern Analysis and Machine Intelligence*, 27(1):115–129, January 2005.